

A Variational Formalism for Excited State Density Functional Theory

Luning Zhao¹ and Eric Neuscamman^{1, 2, a)}

¹⁾*Department of Chemistry, University of California, Berkeley, California 94720, USA*

²⁾*Chemical Sciences Division, Lawrence Berkeley National Laboratory, Berkeley, CA, 94720, USA*

(Dated: 12 May 2022)

We present a formalism for a variational excited state density functional theory with strong parallels to ground state Kohn-Sham theory. In particular, the approach develops density functional expressions for the energies of singly-excited states and combines them with the variational principle from excited state mean field theory. This formalism avoids the need for linear response and the adiabatic approximation and thus addresses both the electron-affinity/ionization-potential imbalance and the need for post-excitation orbital relaxations. In preliminary testing, these features deliver dramatic improvements in charge transfer energies relative to time dependent density functional theory while maintaining accuracy for valence excitations.

I. INTRODUCTION

Density functional theory (DFT)¹ based on the Kohn-Sham (KS) approach² is the most widely used electronic structure method in chemistry, physics, and materials science. Due to its favorable scaling with system size and reasonable accuracy in a variety of different circumstances, DFT is often regarded as one of the most powerful tools for studying the electronic and dynamic properties of materials and medium to large molecules. Although originally formulated for ground states, the development of time-dependent density functional theory (TDDFT)^{3–6} extends DFT’s capability to model excited states based on a linear response (LR) formalism. Numerous applications have shown that TDDFT’s errors for simple valence excitation energies often fall in the range of 0.1 to 0.5 eV, which is impressively close to the performance of high-level quantum chemistry methods such as EOM-CCSD.⁷ With a similar blend of affordability and accuracy as in the ground state, TDDFT has become the most widely used theoretical method for studying electronic excitations in molecules.

Both ground state DFT and TDDFT are formally exact methods. So far, however, the only computationally tractable forms of these methods involve the use of significant approximations. In the ground state theory, the last few decades have seen considerable effort devoted to improvements in approximations for the exchange-correction (xc) functional. Today, a multitude of functionals are in use, ranging from purely local forms like the local density approximation (LDA)⁸ to more complicated empirical fitting approaches such as the Minnesota⁹ and ω B97¹⁰ families of functionals, to forms that seek to recover important piecewise linearity conditions.^{11–13} Generally speaking, the empirical inclusion of exact and range-separated exchange has led to impressively accurate ground state properties, such as binding energies, molecular geometries, and barrier heights.¹⁴ An important point to remember about all of these approaches is that they rely on the KS approximation in which the kinetic energy is evaluated via a fictitious wave function whose form is reasonable for a closed shell ground state. When we consider an analogous

variational formalism for single excitations, it will be natural to attempt to retain this advantage by considering fictitious wave functions whose forms are appropriate for open-shell excitations.

Of course, at present, excitations are usually treated by employing approximate ground state xc functionals in the linear response formalism of TDDFT. This situation arises from the *adiabatic approximation* (AA).^{15,16} The central quantity in TDDFT is the xc-kernel $f_{xc}(\mathbf{r}, t; \mathbf{r}', t')$, defined as the functional derivative of the xc-potential,¹⁵

$$f_{xc}(\mathbf{r}, t; \mathbf{r}', t') = \frac{\delta v_{xc}[n](\mathbf{r}, t)}{\delta n(\mathbf{r}', t')} \quad (1)$$

in which the $v_{xc}(\mathbf{r}, t)$ is the time-dependent analogy of the ground state xc-potential and $n(\mathbf{r}, t)$ is the electron density. The AA replaces the time-dependent xc-potential with the ground state xc-potential¹⁵,

$$v_{xc}^{adia}[n](\mathbf{r}, t) = v_{xc}^{GS}[n(t)](\mathbf{r}) \quad (2)$$

at which point the xc-kernel becomes

$$f_{xc}^{adia}(\mathbf{r}, t; \mathbf{r}', t') = \frac{\delta v_{xc}^{GS}[n(t)](\mathbf{r})}{\delta n(\mathbf{r}', t')} = \delta(t-t') \frac{\delta^2 E_{xc}[n]}{\delta n(\mathbf{r}) \delta n(\mathbf{r}')}. \quad (3)$$

Most notably, this approximation leads the xc-kernel to be local both in time and space if the ground state xc functional is local as in LDA, or local in time but nonlocal in space in the case of hybrid functionals.

While the AA is enormously convenient in that it makes TDDFT efficient and allows it to use existing ground state functionals, it does create important limitations when modeling charge transfer (CT), Rydberg, and double excitations. For example, TDDFT often drastically underestimates excitation energies for long-range CT states^{17–19} and Rydberg states,^{20–22} and it is completely incapable of describing doubly excited states.^{23,24} Besides the underestimation of excitation energies, it is also well known that for long-range CT excited states, standard pure and hybrid functionals also fail to exhibit the correct $1/R$ dependence along the charge separation coordination.^{17,25} Given the technological and biological importance of CT, the limitations of practical TDDFT in this area are especially frustrating.

^{a)}Electronic mail: eneuscamman@berkeley.edu.

To be more precise, these difficulties stem from two approximations: first, the usage of approximate xc functionals, and second, the AA. The former is responsible for the problems in Rydberg excited states and the missing $1/R$ behavior in long-range CT. For Rydberg states, the problem lies primarily in the fact that the ground state xc-potential of local and semi-local functionals decays exponentially with r , much faster than the $1/r$ decay of the exact xc-potential. In order to deal with this problem, the asymptotic correction approach²¹ has been developed and results in dramatically improved Rydberg energetics. For CT excited states, range-separated hybrid functionals (RSH)²⁶⁻³¹ successfully yield the correct $1/R$ behavior of long range CT excited states. These functionals separate the Coulomb potential into a short-range and a long-range part and then gradually switches to a full Hartree-Fock (HF) exchange treatment in the long range limit. This approach eliminates the CT self-interaction error in which derivatives of the approximated exchange term fail to deliver the long range Coulomb term that should be present in the linear response equations.²³ Even with the $1/R$ issue repaired, though, long range CT still poses challenges due to DFT's imbalanced accounting of electron-electron repulsion in the orbital energies that control ionization potentials and electron affinities, a problem we will refer to as the EA/IP imbalance. While we will discuss this issue further when analyzing our results, we will for now point out that substantial progress in this area has been made via the optimal tuning approach,^{32,33} even if it is not always obvious how to select a single tuning parameter in cases where multiple different types of excitations are to be treated simultaneously.

Unlike issues with CT, TDDFT's failure to describe doubly excited states can be laid squarely at the feet of the AA, which converts the memory-dependent time-non-local xc-kernel $f_{xc}(\mathbf{r}, t; \mathbf{r}', t')$ into a time-local affair with no memory. One consequence of this simplification is that, when expressed in Fourier space, the AA xc kernel is frequency independent. Given that it has been shown that the exact xc kernel carries a strong frequency dependence near a double excitation,^{34,35} adiabatic xc-kernels are thus not appropriate or accurate for doubly excited states. In practice, this failure also creates difficulties for other excitations, especially in the context of CT. As pointed out by Ziegler and coworkers,^{36,37} another consequence of the AA is that it fails to account for orbital relaxation effects. An intuitive way to see this in light of the double excitation limitation is to consider that, after the single excitation itself, the leading order term in the Taylor expansion of an orbital-relaxed singly excited state is a linear combination of doubly excited determinants. Since CT excited states undergo substantial charge deformations and changes in dipole when compared to the ground state, allowing the orbitals to relax during the excitation is crucial.³⁸ Without orbital relaxation effects, errors in CT excitation energies often reach multiple eVs,¹⁷ even when RSH functionals are employed. In sum, it would be highly desirable to have a practical excited state DFT methodology that could bypass the AA and so relax orbitals while also resolving the EA/IP imbalance.

In this paper, we present a variational excited state DFT (VES-DFT) in pursuit of this goal. Instead of relying on

the linear response formalism and AA of TDDFT, we develop density functional expressions for the energies of simple excitations and couple them with an excited state variational principle in a manner that strongly parallels the KS-DFT approach to ground states. Excited state variational principles have recently been successfully incorporated into both quantum Monte Carlo³⁹ and excited state generalizations of Hartree Fock theory.^{40,41} By further extending them into DFT, the work presented here addresses both the need for excited-state-specific orbital relaxations and the EA/IP imbalance. In a variety of exploratory calculations, we find that, when paired with an xc functional with a high degree of exact exchange (necessary to help alleviate a self-interaction bias stemming from excited states' more open-shell character), VES-DFT provides an accuracy comparable to TDDFT for simple valence excitations while far outperforming it in CT states, even when comparing against a RSH functional.

This paper is organized as follows. We begin with a brief review of ground state DFT so as to make clear its parallels with our excited state formalism. We then develop the working equations for the VES-DFT method in the context of both single-configurational and multi-configurational fictitious wave functions. We then briefly review the ground state xc functionals that we employ and discuss concerns about possible double counting problems. At the end of the theory section, we compare VES-DFT with other excited state and multi-reference DFT methods and also with constrained DFT. Results and discussions are then presented for a variety of different valence, CT, and Rydberg excitations. We conclude our discussion by pointing out the merits and drawbacks of the current method, along with possible directions for future development.

II. THEORY

A. Ground State DFT

In ground state DFT, the Levy constrained search formulation provides a formally exact energy functional,¹

$$E[n] = \min_{\Psi \rightarrow n} \langle \Psi | \hat{T} + \hat{V}_{ee} | \Psi \rangle + V_{ext}[n] \quad (4)$$

in which \hat{T} and \hat{V}_{ee} are the kinetic and electron-electron repulsion operators, and $V_{ext}[n]$ is the external potential. Practical formulations to KS-DFT approximate this functional as¹

$$E[n] = T_s[n] + V_{ext}[n] + J[n] + E_{xc}[n], \quad (5)$$

in which $T_s[n]$ is the kinetic energy of a fictitious Slater determinant that shares the same density as the actual interacting system, $J[n]$ is the Hartree part of the electron-electron repulsion energy, and $E_{xc}[n]$ is the exchange-correlation functional. Considering the common case of a closed-shell, spin-restricted KS determinant for N electrons, one can re-express the energy in terms of the orbitals $\phi_i(\mathbf{r})$ for $i \in [1, 2, \dots, N/2]$.

The external potential and Hartree pieces,

$$V_{ext}[n] = \int v_{ext}(\mathbf{r})n(\mathbf{r})d\mathbf{r} \quad (6)$$

$$J[n] = \frac{1}{2} \int \frac{n(\mathbf{r})n(\mathbf{r}')}{|\mathbf{r}-\mathbf{r}'|} d\mathbf{r}d\mathbf{r}' \quad (7)$$

are dependent only on the density, which is in turn now determined by the orbitals,

$$n(\mathbf{r}) = 2 \sum_i^{N/2} |\phi_i(\mathbf{r})|^2. \quad (8)$$

Note that we follow the convention that i, j, k refer to occupied orbitals, a, b, c to virtual orbitals, and p, q, r, s to all orbitals. In general, functionals with hybrid components now lead the exchange-correlation to be a direct function of the orbitals,

$$E_{xc}[n] \rightarrow E_{xc}(\phi_1, \phi_2, \dots, \phi_{N/2}), \quad (9)$$

and of course, by design, the kinetic energy is as well.

$$T_s[n] = - \sum_i^{N/2} \int \phi_i(\mathbf{r})\nabla^2\phi_i(\mathbf{r})d\mathbf{r} \quad (10)$$

With this orbital-based formulation, one then minimizes Eq. (5) under the constraint that the orbitals remain orthonormal in order to arrive at the KS orbital eigenvector equation,

$$\hat{F}_{KS} \phi_i = \varepsilon_i \phi_i, \quad (11)$$

in which \hat{F}_{KS} is the KS Fock operator.

Crucially, we note that the same energies, orbitals, and densities are arrived at if one performs the minimization

$$E_{KS} = \min_{\mathbf{X}} \left\{ T_s + V_{ext} + J + E_{xc} \right\} \quad (12)$$

in terms of the elements of the anti-Hermitian matrix \mathbf{X} that transforms some initial orthonormal set of orbitals (such as those that diagonalize the one-electron parts of \hat{H}) into the final KS orbitals.

$$\phi_p(\mathbf{r}) = \sum_q [e^{\mathbf{X}}]_{pq} \phi_q^{(0)}(\mathbf{r}) \quad (13)$$

From this perspective, KS-DFT can be seen as the pairing of a minimally-correlated ansatz (the Slater determinant) and a variational principle (the total energy) in which the energy expression within the latter is replaced by a density functional. To formulate VES-DFT, we will follow this perspective, but with excited-state-appropriate choices for the minimally-correlated ansatz and the variational principle.

B. Variational Excited State DFT: Single-CSF Formalism

Take the variational principle first. Drawing on the strong parallels between HF and DFT, we will import the Lagrangian form of the excited state variational principle used in excited

state mean field (ESMF) theory,⁴¹ which is a generalization of HF theory for excited states.

$$L = \langle \Psi | (\omega - \hat{H})^2 | \Psi \rangle - \boldsymbol{\mu} \cdot \frac{\partial E}{\partial \boldsymbol{\nu}} \quad (14)$$

Here ω is an energy used to select which excited state is being targeted, $\boldsymbol{\nu}$ is the vector of variational parameters within the ansatz, and $\boldsymbol{\mu}$ is a vector of Lagrange multipliers by which we constrain the the minimization of L so that it must converge to an energy stationary point. In essence, the first term in L is a rigorous excited state variational principle with the energy eigenstate closest to ω as its global minimum, but because approximate ansatzes will prevent us from reaching this minimum, we add the energy stationarity constraint to ensure that at least this important property of exact excited states is maintained. In other words, the idea is for the first term to drive the optimization to the energy stationary point that best corresponds to the desired excited state. In preliminary work on ESMF,⁴¹ it has been found that computationally tractable approximations to this Lagrangian

$$\tilde{L} = (\omega - E)^2 - \boldsymbol{\mu} \cdot \frac{\partial E}{\partial \boldsymbol{\nu}} \quad (15)$$

are in practice effective at achieving the same goal, and so for expediency's sake we will adopt \tilde{L} as our working variational principle for VES-DFT.

Before deciding exactly what type of density functional energy expression we should insert into Eq. (15), we should consider the choice of minimally correlated ansatz. To start, consider a singly excited configuration state function (CSF), which is perhaps the simplest spin-pure excited state ansatz.

$$|\Psi_i^a\rangle = \frac{1}{\sqrt{2}} \left(a_a^+ a_i |\Psi_0\rangle \pm a_a^+ a_i^- |\Psi_0\rangle \right) \quad (16)$$

This is a superposition between alpha ($i \rightarrow a$) and beta ($\bar{i} \rightarrow \bar{a}$) excitations from the closed shell Slater determinant Ψ_0 in which the excitations both occur within the same pair of spatial orbitals $\{i, a\}$. The sign determines whether the excitation is a singlet or triplet, and although we will develop the mathematics for the singlet case below, the triplet is equally straightforward. As in the ground state presentation above, the (spin-restricted) molecular orbitals will be defined via an anti-Hermitian matrix \mathbf{X} as in Eq. (13), but with the corresponding ground state KS-DFT orbitals now acting as the initial orbitals $\phi^{(0)}$ and \mathbf{X} encoding excited-state-specific relaxations. This single-CSF ansatz leads to the electron density

$$n_{ia}(\mathbf{r}) = |\phi_a(\mathbf{r})|^2 - |\phi_i(\mathbf{r})|^2 + 2 \sum_k^{N/2} |\phi_k(\mathbf{r})|^2 \quad (17)$$

and a one-body reduced density matrix (1RDM) \mathbf{P} that is diagonal in the basis of the relaxed molecular orbitals.

$$\begin{aligned} P_{kj} &= 2\delta_{kj} - \delta_{ki}\delta_{ji} \\ P_{bc} &= \delta_{ba}\delta_{ca} \\ P_{jb} &= P_{bj} = 0 \end{aligned} \quad (18)$$

As in KS-DFT, we set the kinetic energy to that of the minimally correlated wave function. We express this in the atomic orbital (AO) basis by rotating the 1RDM in to that basis,

$$\mathbf{P}_{AO} = \mathbf{C}_{KS} e^{\mathbf{X}} \mathbf{P} e^{-\mathbf{X}} \mathbf{C}_{KS}^+ \quad (19)$$

where we have used the KS orbital coefficient matrix \mathbf{C}_{KS} . The kinetic energy is then

$$T_{ia} = \langle \Psi_i^a | \hat{T} | \Psi_i^a \rangle = \text{Tr} [\mathbf{P}_{AO} \mathbf{T}_{AO}] \quad (20)$$

with \mathbf{T}_{AO} being the kinetic energy AO integrals,

$$[\mathbf{T}_{AO}]_{pq} = -\frac{1}{2} \int \chi_p(\mathbf{r}) \nabla^2 \chi_q(\mathbf{r}) d\mathbf{r}, \quad (21)$$

and χ_p the AO basis functions. By similarly converting the expression for the density in to the AO basis,

$$n_{ia}(\mathbf{r}) = \sum_{pq} \chi_p(\mathbf{r}) [\mathbf{P}_{AO}]_{pq} \chi_q(\mathbf{r}), \quad (22)$$

the external potential contribution may be evaluated as

$$V_{ia}^{ext} = \text{Tr} [\mathbf{P}_{AO} \mathbf{h}_{AO}], \quad (23)$$

$$[\mathbf{h}_{AO}]_{pq} = \int \chi_p(\mathbf{r}) v_{ext}(\mathbf{r}) \chi_q(\mathbf{r}) d\mathbf{r}. \quad (24)$$

Turning our attention now to the electron-electron repulsion energy, we start with the Hartree term, which for this singlet CSF's density is

$$J[n_{ia}] = \frac{1}{2}(ii|ii) + \frac{1}{2}(aa|aa) - (aa|ii) \\ + 2 \sum_{kj} (kk|jj) + 2 \sum_j \left((aa|jj) - (ii|jj) \right), \quad (25)$$

which we have expressed in terms of the two-electron integrals in the relaxed orbital basis.

$$(pq|rs) = \int \int \frac{\phi_p(\mathbf{r}) \phi_q(\mathbf{r}) \phi_r(\mathbf{r}') \phi_s(\mathbf{r}')}{|\mathbf{r} - \mathbf{r}'|} d\mathbf{r} d\mathbf{r}' \quad (26)$$

For hybrid functionals, we will need a definition for the “exact” wave function based exchange energy, which we choose to arrive at by making the usual index exchanges in the two-electron integrals of the corresponding Hartree term.

$$E_{ia}^{x(\text{wfn})} = -\frac{1}{2}(ii|ii) - \frac{1}{2}(aa|aa) + (ai|ia) \\ - 2 \sum_{kj} (kj|jk) - 2 \sum_j \left((aj|ja) - (ij|ji) \right) \quad (27)$$

When used for a closed shell determinant in the ground state context, this index-exchange approach leads to the familiar situation in which the Hartree and “exact” exchange terms sum to the electron-electron repulsion energy of the Slater determinant. However, things are not so simple in the excited state, and even for this single-CSF singlet wave function, the full wave-function-based electron-electron repulsion energy contains one additional term:

$$E_{ia}^{ee} \equiv \langle \Psi_i^a | \hat{V}_{ee} | \Psi_i^a \rangle = J[n_{ia}] + E_{ia}^{x(\text{wfn})} + (ai|ia). \quad (28)$$

For the triplet CSF, we have a similar situation, but the additional term takes on the opposite sign:

$$E_{ia}^{ee(\text{triplet})} = J[n_{ia}] + E_{ia}^{x(\text{wfn})} - (ai|ia). \quad (29)$$

This extra term, which we will denote as the fictitious system correlation energy (FSCE)

$$E_{ia}^{\text{FSCE}} = \pm (ai|ia), \quad (30)$$

determines the singlet-triplet splitting and arises from the fact that \hat{V}_{ee} connects the two different terms in our CSF. This type of strong correlation effect, in which the electron-electron repulsion is modified by the fact that orbitals i and a are never doubly occupied simultaneously, is simply not present in a closed shell ground state. This fact is important, because it implies that the practical formulations of ground state exchange-correlation functionals that we are about to utilize will not include such an effect, and therefore it should not lead to much double counting if we amend them with this extra strong correlation term. This in mind, we define our single-CSF density functional expression for the energy in Eq. (15) as

$$E_{ia} = T_{ia} + V_{ia}^{ext} + J[n_{ia}] + E_{ia}^{xc} + E_{ia}^{\text{FSCE}} \quad (31)$$

The first three terms are as defined in Eqs. 20, 23, and 25, with the last term providing the strong correlation effect from the spin-pure open shell. The exchange correlation functional is taken as the ground state functional of choice (e.g. B3LYP) but with the density set to n_{ia} and the expression for the exact exchange (if using a hybrid) set to Eq. (27) rather than the ground state Slater determinant expression. As in the ground state theory, in which $E^{\text{FSCE}} = 0$ and HF is recovered by using a functional with no correlation and 100% exact exchange, such a “pure exact exchange” functional leads the present formalism to become the analogous wave function theory based on a single CSF. Thus, in combining Eqs. (15) and (31), we followed the same general approach that leads to KS-DFT in the ground state case. Specifically, we combined a minimally correlated ansatz with a variational principle in which the energy was replaced with that of a density functional.

As in ESMF theory, the minimization of Eq. (15) requires the evaluation of certain sums over energy second derivatives. Although the density functional energy expression of Eq. (31) differs from that of ESMF theory, we can exploit the same automatic differentiation (AD) approach in order to perform the optimization at a cost whose scaling with system size is the same as a ground state KS Fock build. For an explanation of how this is achieved, we refer the reader to the original ESMF paper.⁴¹ As in that case, we have formulated our pilot code using the convenient AD capabilities of the TensorFlow framework⁴² and have carried out the minimization via a quasi-Newton approach.⁴³

C. Variational Excited State DFT: Multiple-CSF Formalism

In cases where a state contains major contributions from multiple different single excitations, we may generalize the

approach into a multi-CSF form with a wave function similar to configuration interaction singles (CIS),⁴⁴

$$|\Psi_{\text{MCSF}}\rangle = \sum_{ia} c_{ia} |\Psi_i^a\rangle, \quad (32)$$

in which we still relax the orbitals as above. In this case, the density becomes

$$\begin{aligned} n_{\text{MCSF}}(\mathbf{r}) = & 4 \sum_{ia} |c_{ia}|^2 \sum_k |\phi_k(\mathbf{r})|^2 + 2 \sum_{iab} c_{ia} c_{ib} \phi_a(\mathbf{r}) \phi_b(\mathbf{r}) \\ & - 2 \sum_{ija} c_{ia} c_{ja} \phi_i(\mathbf{r}) \phi_j(\mathbf{r}) \end{aligned} \quad (33)$$

and the 1RDM in the relaxed MO basis is no longer diagonal.

$$\begin{aligned} P_{ij} &= \delta_{ij} - \sum_a c_{ia} c_{ja} \\ P_{ia} &= P_{ai} = 0 \\ P_{ab} &= \sum_i c_{ia} c_{ib} \end{aligned} \quad (34)$$

Nonetheless, we can still take the KS approach and evaluate both the kinetic energy and external potential via the wave function's 1RDM using Eqs. (20) and (23).

Although the one-electron components are quite similar to the single-CSF approach, the electron-electron repulsion energy is less straightforward. In order to define the Hartree term, one possibility is to use the density from Eq. (33) in the standard $J[n]$ form of Eq. (7). However, doing so introduces unphysical virtual-virtual Coulomb repulsion terms in the form of $(aa|bb)$, similar to the ghost interactions encountered in ensemble DFT. In order to avoid these in the multi-CSF case, we generalize the Hartree term as the weighted statistical average of the Hartree terms from each separate CSF as given in Eq. (25).

$$J_{\text{MCSF}} \equiv \sum_{ia} |c_{ia}|^2 J[n_{ia}] \quad (35)$$

If we now apply the index-exchange approach, we simply arrive at an ‘‘exact’’ wave function exchange that is the weighted average of the single-CSF pieces from Eq. (27).

$$E_{\text{MCSF}}^{x(\text{wfn})} \equiv \sum_{ia} |c_{ia}|^2 E_{ia}^{x(\text{wfn})} \quad (36)$$

As before, the Hartree and exchange pieces do not add up to the full wave function electron-electron repulsion energy,

$$\langle \Psi | \hat{V}_{ee} | \Psi \rangle = J_{\text{MCSF}} + E_{\text{MCSF}}^{x(\text{wfn})} + E_{\text{MCSF}}^{\text{FSCE}}, \quad (37)$$

and the additional correlation effects are now more involved.

$$\begin{aligned} E_{\text{MCSF}}^{\text{FSCE}} = & 2 \sum_{iajb} c_{ia} c_{jb} [2(ai|jb) - (ab|ji)] \\ & + \sum_{abi} c_{ia} c_{jb} \left[\sum_k 4(ab|kk) - 2(ak|kb) \right] \\ & - \sum_{ija} c_{ia} c_{ja} \left[\sum_k 4(ij|kk) - 2(jk|ki) \right] \\ & + \sum_{ia} |c_{ia}|^2 \sum_k [-4(aa|kk) + 2(ak|ka) + 4(ii|kk) - 2(ik|ki)] \\ & + \sum_{ia} |c_{ia}|^2 [2(aa|ii) - 2(ai|ia)] \end{aligned} \quad (38)$$

Using the same logic as before (although see Section II E regarding double counting concerns), we define the multi-CSF density functional form for the energy in Eq. (15) to be

$$E_{\text{MCSF}} = T + V_{\text{ext}} + J_{\text{MCSF}} + E_{xc} + E_{\text{MCSF}}^{\text{FSCE}} \quad (39)$$

in which the T and V_{ext} are as in Eqs. (20) and (23) but with the multi-CSF 1RDM, and E_{xc} is as in the ground state functional but with the density taken from Eq. (33) and the ‘‘exact’’ exchange component set to $E_{\text{MCSF}}^{x(\text{wfn})}$. Although this definition is not unique due to our somewhat arbitrary choice for the Hartree and exchange terms, it does offer three advantages. First, unphysical virtual-virtual repulsions are avoided. Second, as in both KS-DFT and our single-CSF formalism, setting the xc functional to 100% exact exchange with no correlation recovers the wave function theory, which in this case is ESMF theory.⁴¹ Third, as in KS-DFT, each term that results from expanding Eq. (35) has a direct classical interpretation.

D. Exchange Correlation Functionals

So far we haven't discussed the specific form of E_{xc} . In the current study we use the following three different xc functionals: LDA, the Becke3-Lee-Yang-Parr functional,⁴⁵⁻⁴⁷ and the Becke-Half-Half.⁴⁸ Their xc functionals are:

$$E_{xc}^{\text{LDA}}[n] = E_x^{\text{UEG}}[n] + E_c^{\text{UEG}}[n] \quad (40)$$

$$\begin{aligned} E_{xc}^{\text{B3LYP}}[n] = & 0.08E_x^{\text{UEG}}[n] + 0.72E_x^{\text{B88}}[n, \nabla n] + 0.2E_x \\ & + 0.81E_c^{\text{LYP}}[n, \nabla n, \nabla^2 n] + 0.19E_c^{\text{UEG}}[n] \end{aligned} \quad (41)$$

$$\begin{aligned} E_{xc}^{\text{BHHLYP}}[n] = & 0.5E_x^{\text{B88}}[n, \nabla n] + 0.5E_x \\ & + 0.81E_c^{\text{LYP}}[n, \nabla n, \nabla^2 n] + 0.19E_c^{\text{UEG}}[n] \end{aligned} \quad (42)$$

in which $E_x^{\text{UEG}}[n]$ and $E_c^{\text{UEG}}[n]$ are the exchange and correlation energy of the uniform electron gas (UEG) with density n . E_x^{B88} is the B88 generalized gradient approximation (GGA)⁴⁷ to the exchange energy. E_c^{LYP} is the LYP GGA⁴⁵ to the correlation energy. E_x is the exact exchange energy defined in either Eq. (27) or (36). One could see that a major difference in these three functionals is the amount of exact exchange mixing: 0% for LDA, 20% for B3LYP, and 50% for BHHLYP. We test a range of these because we expect the exact exchange fraction to matter, as the ground and excited states have different amounts of open shell character and thus are likely to suffer from differing degrees of self-interaction error. Choosing an exact exchange fraction that best avoids a bias resulting from such self-interaction imbalance will be important, and since existing functionals were optimized for the closed shell state, it will not be surprising if a higher than usual fraction is necessary to create a fair playing field for the open-shell state. That said, we should be clear that when evaluating excitation energies, the same xc functional with the same exact exchange fraction is used for both the ground and excited state formalisms. The difference between ground and excited state evaluation is simply that the former is treated with KS-DFT while the latter is treated with VES-DFT.

E. Double Counting Problems

The VES-DFT energy, in both the single and multiple CSF formalisms, contains correlation terms that do not exist in the energy expression of ground state DFT. However, one potential problem of adding these correlation terms into the energy formula as we have done is that, in principle, they could be accounted for again in the xc functional, leading to a double counting problem. In the single-CSF formalism, the FSCE term ($ai|ia$) arises completely due to the fact that the wave function contains two determinants with equal weights. Otherwise, the overall spin-symmetry would be broken and singlet-triplet gaps incorrect. Such a strong correlation effect is (typically) not built in to practical forms for E_{xc} which instead aim to include weak correlation effects.⁴⁹ Therefore, we do not expect to have significant double counting problems in the single-CSF case.

However, if one employs the full CIS-style multi-CSF formalism, the wave function definitely includes some weak correlation effects. In order to illustrate this, consider the case where the multi-CSF expansion is dominated by one CSF with an excitation between the i th and a th orbitals. We can treat such a dominated piece as the zeroth-order reference in a perturbative expansion. As the other (symmetry-allowed) singly-excited CSFs are coupled to this reference by \hat{V}_{ee} , their coupling would be part of any 2nd-order perturbation correction starting from this reference. Thus, a simple Moller-Plesset-style argument suggests that many and perhaps most of the contributions within E_{MCSF}^{FSCE} would be part of the system's weak correlation physics and so at significant risk of double counting within our multi-CSF formalism. Indeed, in early testing, we found that excitation energies with the full multi-CSF formalism were worse than those from the single-CSF formalism, which we now understand was primarily a double counting issue.

In order to avoid this problem, one might try to separate contributions from the weak and strong correlations within the multi-CSF expansion. Although there is no unique way to do this, we have for now taken the expedient approach of including in our multi-CSF expansion only those CSFs whose TDDFT coefficients are above a threshold. While it may become clear once more data is available what the least-bad threshold choice would be, we have for now set this threshold at a relatively large value of 0.2 to help ensure that retained CSFs are playing a larger-than-perturbative role in the excitation and are therefore more likely to contribute energetic correlation effects of the type that are not built in to common density functionals. For simplicity, and in contrast to ESMF theory, we do not optimize these coefficients in our minimization of \tilde{L} and instead hold them fixed at their TDDFT values.

F. Comparison to multi-reference DFT

The VES-DFT uses an inherently multi-referenced wave function to evaluate the kinetic energy. Such an approach resembles various multi-reference (MR) DFT methods, such as MRCI/DFT,⁵⁰ multiconfiguration Pair-Density Functional

Theory (MC-PDFT),^{51,52} and density matrix renormalization group pair-density functional theory (DMRG-PDFT).⁵³ As in VES-DFT, both MC-PDFT and DMRG-PDFT use a multi-referenced wave function to evaluate the kinetic energy and the classical Coulomb energy. Also like VES-DFT, MR-DFT methods must be wary of double counting correlation. However, unlike our current approach to VES-DFT, which makes a rough attempt to separate weak and strong correlation, MC-PDFT and DMRG-PDFT take a different route. In MC-PDFT and DMRG-PDFT, the MR wave function is only used to compute the kinetic and classical Coulomb energy, with all correlation effects handled by the on-top pair density functional.⁵⁴ This functional, unlike the more traditional xc functionals used in KS-DFT, contains contributions from two-electron density matrices and can thus more effectively evaluate both both strong and weak correlation effects within the functional itself.

Although VES-DFT thus has some strong parallels with existing forms of MR-DFT, it also possesses several advantages. Perhaps most importantly, current MR-DFT formulations rely on ground state orbitals and do not relax them during the DFT calculation. In contrast, the use of an approximate excited state variational principle allows VES-DFT to relax the orbital basis for each individual excited state. Another advantage is that, by design, VES-DFT shares the same cost scaling with system size as ground state KS-DFT. Once implemented at production level, this trait should facilitate applications in larger systems. Current approaches to MR-DFT, on the other hand, are limited by the exponential scaling of CASSCF, MRCI, and DMRG. That said, paying this price does confer the ability to treat states such as double excitations that are clearly out of reach of our initial VES-DFT formulation, so this comparison is not entirely straightforward. Finally, a second key advantage deriving from the use of an excited state variational principle is that VES-DFT can in principle be applied to excited states deep in the energy spectrum without increasing its computational cost. Current MR-DFT methods rely on Krylov-style diagonalizations that must also resolve the lower roots of the Hamiltonian when aiming at a highly excited states.

G. Comparison to non-TDDFT Excited State DFT Methods

Certainly VES-DFT is not the first DFT method that allows for excited-state-specific orbital relaxation. Δ self-consistent field DFT (Δ SCF)⁵⁵ relaxes excited state orbitals by searching for open-shell solutions to the single-determinant KS-DFT energy stationary conditions. While this approach can be very effective, it is prone to variational collapse, in which the SCF optimization converges back to the ground state determinant. Although it does not always succeed, the the maximum overlap method (MOM)^{56,57} can overcome the collapse issue in many cases, allowing MOM-based Δ SCF to succeed in some particularly challenging settings such as core excitations.⁵⁷

Another approach to relaxing orbitals while avoiding collapse to the ground state that also mitigates the lack of spin purity in Δ SCF is the restricted open-shell Kohn-Sham (ROKS)

method.^{58,59} Compared to Δ SCF, ROKS is for example better positioned to produce accurate singlet-triplet splittings in CT excitations.⁵⁹ However, since it is still the energy that ROKS tries to minimize, it is still prone to a variational collapse problem. While its open-shell nature of course prevents it from collapsing to the ground state, ROKS must still contend with the problem of collapsing to a lower excited state of the same symmetry. In contrast, the VES-DFT approach minimizes an excited state variational principle, and so should be less prone to collapse issues, at least in principle. That said, as a non-linear optimization method, VES-DFT is only guaranteed to converge to the desired energy stationary point if the initial guess is within its radius of convergence, and so in practice the question of whether it faces issues analogous to variational collapse will need to be investigated carefully. The preliminary tests we present below are clearly not exhaustive enough to settle this issue, but we will say that we have not encountered any collapse-like behavior in our calculations so far. Another clear difference from both Δ SCF and ROKS is that the multi-CSF formalism for VES-DFT allows it to study states that strongly mix two or more excitation components.

H. Comparison to Constrained DFT

The constrained DFT (CDFT) method⁶⁰ represents another route towards obtaining accurate predictions for CT excited states. As the name suggests, CDFT performs a ground state DFT calculation with a constraint. For CT states, the constraint is usually chosen to force the right number of electrons on the acceptor in the CT excited states. Because of the constraint, the energy minimization cannot collapse back to the neutral ground state. It has been shown that in various applications involving CT excited states, CDFT gives accurate results in terms of excitation energies,⁶¹ coupling elements,⁶² forces,⁶³ and diabatic surfaces⁶⁴ for electron transfer.

VES-DFT has some strong similarities to CDFT but also important differences. Conceptually, both methods can optimize orbitals specifically for excited states, and both methods modify the optimization in order to guide it to the desired excited state. In CDFT, this guidance comes by constraining a certain region of space to have a given number of electrons. In VES-DFT, an approximated excited state variational principle is employed, which in the form used here simply imparts a preference for energies close to ω . A key difference between these approaches is that while the CDFT constraint is rigid (the final density is forced to satisfy the specified charge constraint exactly even if the true density does not), the energetic nudge in VES-DFT does not force any particular structure on the final density. Indeed, it merely aids in converging to the energy stationary point corresponding to the desired state. Unlike VES-DFT, CDFT's final results will not lie at an energy stationary point and will in general depend on the details of the user-specified constraint.

One very strong parallel that should be emphasized is that VES-DFT and CDFT are mathematically identical for long range CT excitations in which there is no ambiguity in how to define CDFT's charge constraint (see for example Figure 1).

In order to illustrate this, consider that both methods are given the same set of orbitals and the charge transfer is from the HOMO of the donor to the LUMO of the acceptor. Enforcing the additional electron on the acceptor in CDFT is then equivalent to promoting one electron from the donor's HOMO to the acceptor's LUMO. Therefore CDFT and VES-DFT in the single-CSF formalism have the same orbital occupation, leading to the same density, kinetic energy, and external potential. Since the electron densities are the same, VES-DFT and CDFT would yield the same Coulomb repulsion and xc energy. Although in VES-DFT the additional FSCE is added to the total energy, this term vanishes for long range CT, and so CDFT and VES-DFT should produce identical results in this special case.

In shorter-ranged CT, VES-DFT has the formal advantage of not needing to know the final charge on any region in advance, which implies that it has the potential to identify the donor and acceptor orbitals for itself without user-supplied charge constraints. This feature should be especially desirable when one is trying to predict where charge comes from or goes to and also avoids the ambiguities inherent to assigning formal atomic charges that can lead to significant errors in CDFT.⁶⁰ So long as an accurate approximation is employed for the exchange correlation functional — which is the same basic assumption in all uses of ground state DFT — VES-DFT should successfully identify the donor and acceptor for itself without any intervention on the user's part and without the need to assign formal atomic charges.

III. COMPUTATIONAL DETAILS

The calculations in the current study are performed on the following molecular and atomic systems:

- 1) singlet and triplet $n \rightarrow \sigma^*$ excitation in H_2O .
- 2) singlet and triplet $n \rightarrow \pi^*$ excitation in CH_2O .
- 3) singlet and triplet $\sigma \rightarrow \sigma^*$ excitation in LiH.
- 4) singlet He $1s \rightarrow \text{Be } 2p$ excitation in He-Be dimer.
- 5) singlet NH_3 $2p_z \rightarrow \text{F}_2$ $2p_z$ excitation in $\text{NH}_3\text{-F}_2$ dimer.
- 6) singlet $2s \rightarrow 3p_z$ excitation in Ne atom.

All of the VES-DFT results are obtained via our own pilot code, which extracts one- and two-electron integrals from PySCF.⁶⁵ The Lebedev-Laikov grid⁶⁶ is used to perform the numerical integration to compute the xc energy. The TDDFT and CIS results were obtained from QChem.⁶⁷ Equation-of-Motion Coupled Cluster with singles and doubles (EOM-CCSD) results were computed by MOLPRO.⁶⁸ In the current study, the CSF expansions in both single-CSF formalism and multiple-CSF formalism are selected by the CI vector of TDDFT using the same xc functional. Because we choose a large threshold of $\epsilon = 0.2$ for CSF truncation, the single-CSF formalism of VES-DFT is applied to all calculations except the triplet excited state of LiH, in which this threshold leads to the inclusion of 2 CSFs.

In H_2O the H-O-H bond angle is chosen to be 104.5° and the O-H bond length is 0.96\AA . In CH_2O the H-C-H bond angle is 116° , and the C-H and C-O bond length are 1.11\AA and 1.21\AA respectively. In LiH the bond length is 1.6\AA , and the

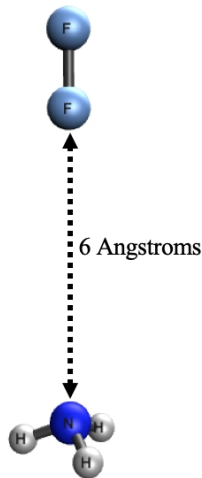


FIG. 1. Geometry of the $\text{NH}_3\text{-F}_2$ dimer. The N-H bond length and H-N-H bond angle is 1.02\AA and 106.2° . The F_2 bond length is 1.43\AA .

He-Be separation is 3.5\AA . The geometry of the $\text{NH}_3\text{-F}_2$ dimer is shown in Figure 1. For basis sets, we employed the cc-pVDZ basis⁶⁹ for H_2O , CH_2O , and LiH , the cc-pVTZ basis⁷⁰ for the He-Be dimer, the aug-cc-pVTZ basis⁷⁰ for Ne, and the 6-31G basis⁷¹ for the $\text{NH}_3\text{-F}_2$ dimer.

IV. RESULTS AND DISCUSSION

A. Excited State Dipole Shifts

Before presenting the results of VES-DFT, we first categorize the excited states into CT and non-CT types by computing the difference between the ground and excited state dipole moment. In atomic units, the dipole moment is

$$\vec{\mu} = \sum_A Z_A \mathbf{R}_A - \int \mathbf{r} n(\mathbf{r}) d\mathbf{r} \quad (43)$$

in which Z_A and \mathbf{R}_A are the charge and position of the A th nuclei. For simplicity, the electron density for excited states is estimated using Equation 17 using ground state KS orbitals without any relaxation. The dipole moment difference ($|\Delta\vec{\mu}|$) between the ground and excited state yields information about the electron charge distribution between these two states.

The computed $|\Delta\vec{\mu}|$ s are shown in Figure 2. For Ne, H_2O , and CH_2O the $|\Delta\vec{\mu}|$ are fairly small, indicating that the charge distributions are similar for the ground and excited states. Thus, these excited states are purely Rydberg (Ne) and valence excited states (H_2O and CH_2O) with little charge deformation. As expected, the long-range CT excited states^{25,72} of He-Be and $\text{NH}_3\text{-F}_2$ have a significantly larger $|\Delta\vec{\mu}|$. Interestingly, the excited state of LiH is also accompanied by a significant amount of charge deformation and a large $|\Delta\vec{\mu}|$ value. This is a consequence of the ionic nature of LiH , in which the bonding and anti-bonding orbitals are shifted towards opposite ends of the molecule. We now discuss each class of

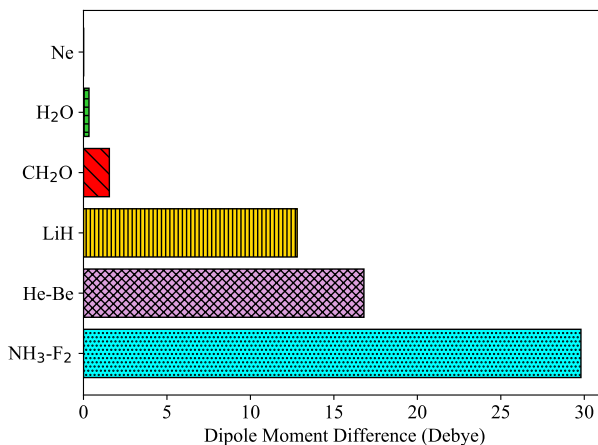


FIG. 2. The norms of the dipole moment differences between ground and excited states. The BHHLYP functional is used in all dipole calculations.

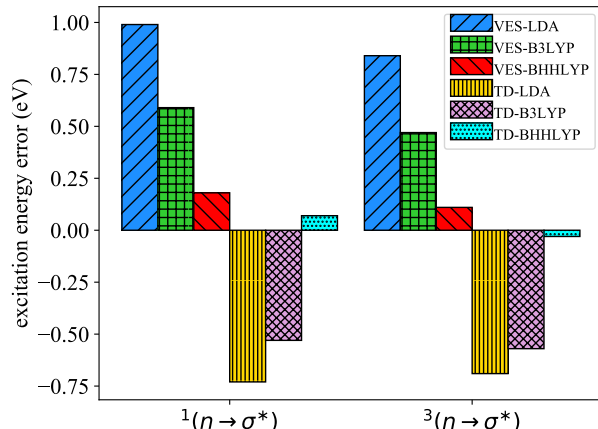


FIG. 3. The excitation energy error of singlet (left) and triplet (right) $n \rightarrow \sigma^*$ excited states in H_2O compared to EOM-CCSD results.

excitations separately, beginning with valence excitations and then moving on through CT and finally Rydberg.

B. Valence Excitations

Excitation energy errors relative to EOM-CCSD for H_2O and CH_2O are shown in Figures 3 and 4, respectively. Compared to the CT examples in the next section, TDDFT performs relatively well for these valence excitations, with B3LYP and especially BHHLYP providing excitation energies within about half an eV of the reference and LDA performing only a little worse. These relatively good TDDFT results are not particularly surprising in light of the fact that the charge density deformations are small, and so the lack of orbital relaxation due to the AA is not especially concerning. In fact, we have explicitly analyzed the importance of orbital relax-

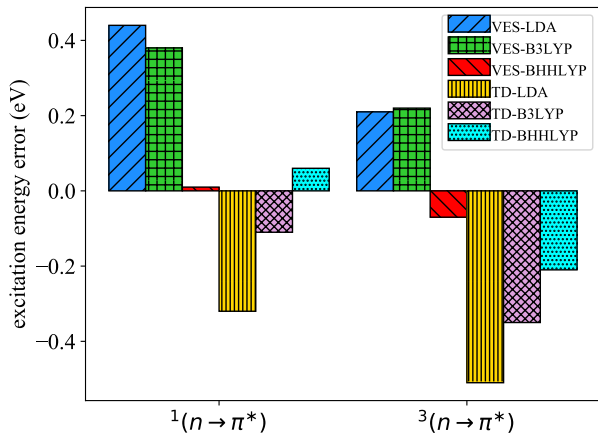


FIG. 4. The excitation energy error of singlet (left) and triplet (right) $n \rightarrow \pi^*$ excited states in CH_2O compared to EOM-CCSD results.

ation by evaluating the Frobenius norm of the VES-DFT orbital rotation matrix \mathbf{X} . Averaging over the three values from the three different functionals tested, we find $\|\mathbf{X}\|$ to be 0.16 and 0.15 for H_2O and CH_2O , respectively, which is smaller than in the CT examples we will see below.

The basic trend in VES-DFT accuracies for different functionals follows that of TDDFT in these excitations, with BHLYP giving the most accurate predictions, followed by B3LYP and then LDA. As we will see, this accuracy ordering for functionals in VES-DFT is seen in every one of our test systems, regardless of whether the excitation is valence, CT, or Rydberg. Our understanding of this across-the-board trend is that a larger degree of exact exchange is most likely helping to balance self-interaction errors in the ground and excited states. We expect that for a given fraction of exact exchange, these errors are larger in the excited states due to their open-shell nature, and so a higher degree of exact exchange than is typically used in ground state models appears to be helpful for balancing these errors between the ground and excited states. We should emphasize that in all of our VES-DFT results, energy differences were evaluated based on the same functional for both ground and excited states, but using the density and “exact” wave function exchange definition for the state in question (see discussion surrounding Eq. (31)). Although future work will clearly need to explore the choice and design of functionals in VES-DFT more systematically, the use of BHLYP achieves errors below 0.2 eV in all four of these initial valence excitation tests, providing an encouraging proof of principle.

C. Charge-Transfer Excitations

Although VES-DFT and TDDFT provide similar accuracies in the simple valence excitations discussed above, the story is very different for CT excitations. Before looking in detail at the numerical CT examples, it is worth considering

two important potential sources of error TDDFT faces in CT contexts, which we will refer to as the EA/IP imbalance and the orbital relaxation error. To see these clearly, consider a simple CT excitation consisting of a single $i \rightarrow a$ transition, in which case the TDDFT excitation energy is given by⁷³

$$\Delta E(i \rightarrow a) = \epsilon_a^{KS} - \epsilon_i^{KS} + \langle ia | f_{xc} | ia \rangle \quad (44)$$

in which ϵ_i^{KS} and ϵ_a^{KS} are the ground state KS orbital energies of the donor and acceptor orbitals, respectively. As is well known in the context of the absence of a formal Koopman’s theorem for electron affinities in KS-DFT, the KS-DFT orbital energies for virtual orbitals localized on an N -electron subsystem only include electron-electron repulsion effects from $N - 1$ electrons.⁴ This contrasts with HF theory, where these virtual orbital energies include repulsion effects from N other electrons and a formal electron affinity Koopman’s theorem is in force. For occupied orbitals localized on an N -electron fragment, the orbital energies of both DFT and HF include $N - 1$ electrons’ worth of repulsion effects and both thereby have a sound formal Koopman’s theorem for ionization energies. Thus, for systems with cleanly separated donor and acceptor, the orbital energy difference in Equation 44 under-estimates the additional electron-electron repulsion arising within the acceptor upon electron attachment but accounts more correctly for the reduction in electron-electron repulsion within the donor upon ionization. This EA/IP imbalance will thus tend to push TDDFT towards too-low excitation energies in long-range CT. Ideally, the third term in Equation 44 would correct this error, but in CT this term is typically small or vanishing for a local functional due to the small or vanishing overlap between the donor and acceptor orbitals. Hybrid functionals do make a non-zero correction via their exact exchange component, but as exact exchange fractions are typically chosen below about 50%, one would not expect this correction to resolve more than half of the EA/IP imbalance. Note especially that range-separated hybrids are not designed to assist with this issue, as it arises from a mismatch in the treatment of intra-donor and intra-acceptor electron-electron repulsion, which in many cases is a short-ranged affair. Instead, the simplest approaches to range-separation help capture electron-hole attraction between the donor and acceptor, and although this is important, it leaves the EA/IP imbalance unresolved. The optimal tuning approach is more effective here, although it is not obvious how it should be generalized to provide a balanced treatment of both valence and CT excitations. In practice, of course, there will also be excitations that fall somewhere in between these two clear-cut categories, which we would expect to further confuse the choice of tuning parameter.

While the EA/IP imbalance is a significant concern, it is typically offset in practice by the fact that TDDFT works with unrelaxed orbitals. As orbital relaxations in the excited state are expected to lower the energy of the acceptor orbital and raise the energy of the donor orbital, the orbital relaxation error arising from the lack of these effects will work to push excitation energies upwards. Ideally, the third term in Equation 44 would eliminate both orbital relaxation issues and the EA/IP imbalance, but even when the third term is zero,

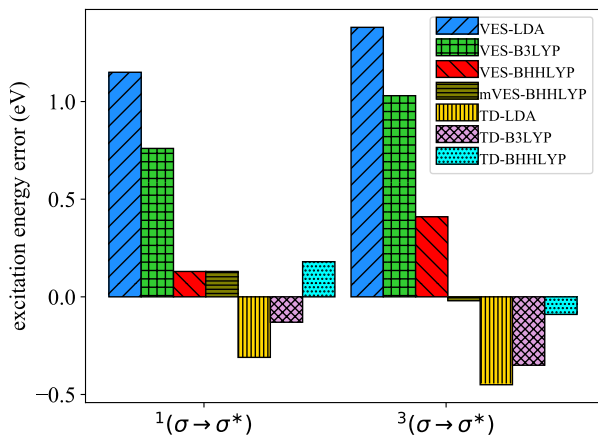


FIG. 5. The excitation energy error of singlet (left) and triplet (right) $\sigma \rightarrow \sigma^*$ excited states in LiH compared to EOM-CCSD results.

these two errors do at least work to cancel each other because they push in opposite directions. However, the EA/IP imbalance in long-range CT is often much too large for orbital relaxation errors to counteract, resulting in TDDFT excitation energies that are much too low as in the $\text{NH}_3 \rightarrow \text{F}_2$ and $\text{He} \rightarrow \text{Be}$ transitions shown below. However, as one moves to increasingly shorter range CT with correspondingly larger overlaps between the donor and acceptor, the EA/IP imbalance becomes less and less of an error and more and more a positive feature of the TDDFT formalism. Indeed, in the valence excitation limit, the difference in how DFT accounts for electron-electron repulsion energy in the occupied and virtual orbitals increases the accuracy of using orbital energy differences as excitation energy estimates, because in this limit the “donor” and “acceptor” are one and the same. One can imagine that for very short-ranged CT, any small remaining errors from the EA/IP imbalance could cancel with orbital relaxation errors precisely enough for the exchange correlation term to clean up the details. Such an effect seems to be at work in LiH, to which we now turn our attention, which despite having a substantial dipole change and thus CT is nonetheless treated well by TDDFT.

1. LiH

Figure 5 shows excitation energy errors for the lowest singlet and triplet excitations in LiH. For both of these states, the balancing process between EA/IP issues and missing orbital relaxations appears to work in TDDFT’s favor, especially in the case of the BHLYP functional. To check that such a trade off really does appear to be at work here, we again evaluated $\|\mathbf{X}\|$ as a measure of orbital relaxation importance and found it to be 0.41, significantly higher than for H_2O or CH_2O . As in the valence states of those molecules, BHLYP is also very effective in VES-DFT’s single-CSF formalism for LiH’s singlet excitation. For the triplet, however, the

single-CSF formalism shows relatively poor accuracy regardless of functional, and indeed this is the one state among those tested so far in which there are more than one CSFs above our $\epsilon = 0.2$ threshold in TDDFT. When we include both of the CSFs whose coefficients breach this threshold via the multi-CSF approach, the VES-DFT/BHLYP result improves from an error above 0.4 eV to an error of just -0.02 eV relative to EOM-CCSD. Note that the multi-CSF approach has no effect on the singlet state, as in that case only the primary CSF was above the threshold.

2. NH_3 to F_2

We now turn our attention to the first of two long-range CT excitations: the $\text{NH}_3\text{-F}_2$ dimer shown in Figure 1. In Figure 6, we see that, after excited-state orbital relaxation via the minimization of Eq. (15), VES-DFT is substantially more accurate than TDDFT regardless of the functionals chosen. Even when comparing VES-DFT/LDA against TDDFT with the ωB97X RSH, the variational approach makes an excitation energy error roughly half as large. Using BHLYP, which continues to outperform the others for VES-DFT, the variational approach achieves an excitation energy error of just 0.26 eV, compared to about 4 eV for TDDFT with either ωB97X or BHLYP.

It would appear that TDDFT’s error cancellation between its EA/IP imbalance and its lack of orbital relaxations breaks down here, with the magnitude of the former overwhelming that of the latter. We can verify this picture in two ways: first, with the VES-DFT approach, and second, by looking at ground state KS-DFT IP-EA estimates at very long range. Start with VES-DFT. At the top of Figure 6, we show the excitation energies (i.e. the energy differences between Eq. (31) and the ground state KS energy) *before* the VES-DFT orbital optimization has been carried out, meaning that the excited state VES-DFT energy is being evaluated using the ground state KS orbitals. This excitation energy is thus the difference between two many-electron DFT energies (one VES-DFT and one KS-DFT) and so does not suffer from the EA/IP imbalance that arises in the difference between KS single-particle orbital energies. While the EA/IP issue has thus been removed, orbital relaxation effects have yet to be included, and as expected the excitation energies are now too large. When we then relax the orbitals ($\|\mathbf{X}\| = 0.21$), we see in the middle of Figure 6 that the predicted excitation energies decrease to more accurate values. Thus, by looking step-wise at how VES-DFT changes the energy from TDDFT, we can watch the staged removal of first the EA/IP imbalance and then the fixed-orbital error. This process appears to confirm the idea that TDDFT suffers from both, and that in long-range CT the EA/IP part dominates, leading TDDFT to underestimate the excitation energy.

We can corroborate this view by moving the molecules to a very large distance and comparing VES-DFT, TDDFT, and a simple difference of ground state KS energies between the cation, anion, and neutral species that provides a many-electron evaluation of the IP and EA. At very long distance, Figure 7 shows that the performance of VES-DFT and

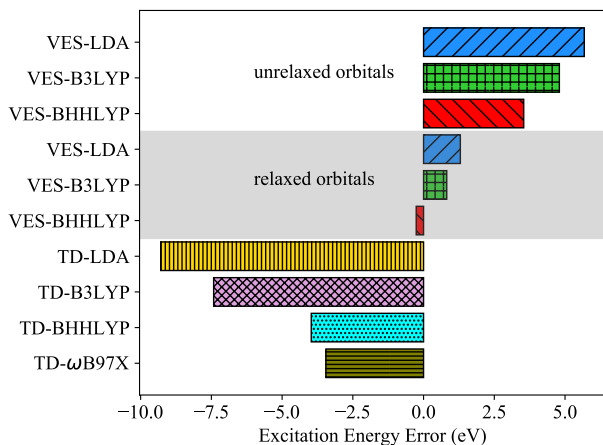


FIG. 6. Comparison of excitation energy errors relative to EOM-CCSD for the NH_3 $2\text{pz} \rightarrow \text{F}_2$ 2pz CT excitation at an intermolecular separation of 6 \AA . For VES-DFT, we show the results both before and after the orbital relaxation is performed.

TDDFT is quite similar to what we saw at the shorter separation. At the bottom of the figure, we see that if we simply perform four single-molecule ground state KS calculations for the donor cation, acceptor anion, and the two neutral species, the resulting difference between the IP and EA is a very accurate predictor of the charge transfer energy, as we would expect from previous work on CDFT. Thus, if both the IP/EA imbalance born of single-particle orbital energy differences and the orbital relaxation errors are removed via this ground state KS approach or by CDFT, accuracy is restored. The key point is that, unlike these approaches, the VES-DFT formalism should allow both of these issues to be addressed even in systems where clear-cut foreknowledge distinguishing between the donor and acceptor is not available.

3. He to Be

In our second long-range CT example, we investigate the excitation from the He $1s$ orbital to the Be 2pz orbital as a function of the distance between the atoms. In Figure 8, we see the familiar failure of local functionals and simple hybrids to predict the correct $1/R$ trend in the excitation energy. While this problem is repaired by the use of a RSH, we see that absolute accuracy is still poor, at least for the specific ωB97X functional we tested here. As in the previous example, VES-DFT outperforms the accuracy of the RSH regardless of which functional it is paired with while also correctly capturing the $1/R$ behavior. The advantage of VES-DFT becomes especially clear when looking at the non-parallelity error (NPE) plotted in Figure 9, which is defined as the difference between the largest and smallest errors relative to EOM-CCSD across the distance coordinate. VES-DFT with LDA, B3LYP, and BHLYP all produce NPEs below 1eV , as compared to an NPE of almost 2eV for TDDFT with the ωB97X functional.

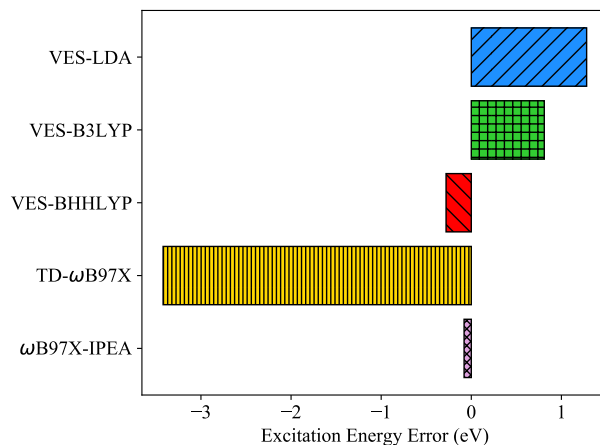


FIG. 7. Excitation energy errors relative to EOM-CCSD for the NH_3 $2\text{pz} \rightarrow \text{F}_2$ 2pz CT at a 120 \AA intermolecular separation. $\omega\text{B97X-IPEA}$ refers to the difference between (a) the sum of ground state KS energies for the donor cation and acceptor anion and (b) the ground state KS energy of the neutral ground states.

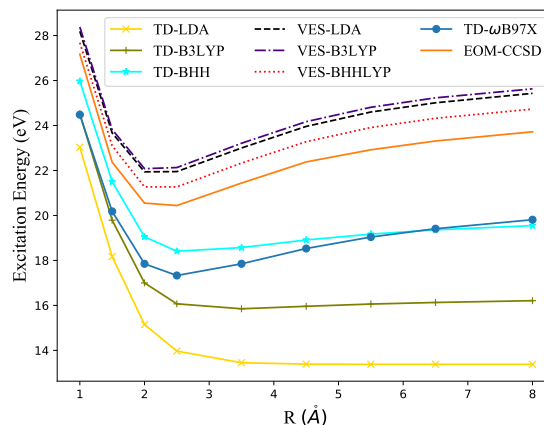


FIG. 8. Comparison of He $1s \rightarrow \text{Be}$ 2p CT excitation energy as a function of $R(\text{He-Be})$ between VES-DFT, TDDFT, and EOM-CCSD.

As in the $\text{NH}_3\text{-F}_2$ transition, both the EA/IP imbalance and orbital relaxations appear to be important in this system. Averaged across the distance coordinate, the norm of the VES-DFT orbital rotation matrix that we are using as a metric for the importance of orbital rotations is $\|\mathbf{X}\| = 0.3$, which is higher than in either of our valence excitation examples. Given that TDDFT errors low relative to EOM-CCSD and that VES-DFT errors high (even after orbital relaxation), we again conclude that in TDDFT the EA/IP imbalance error is overwhelming the orbital relaxation error at all distances. By addressing both of these errors, VES-DFT does not rely on them cancelling each other, and so produces a more accurate picture than can be achieved within the linear response formalism when limited to practical functional forms.

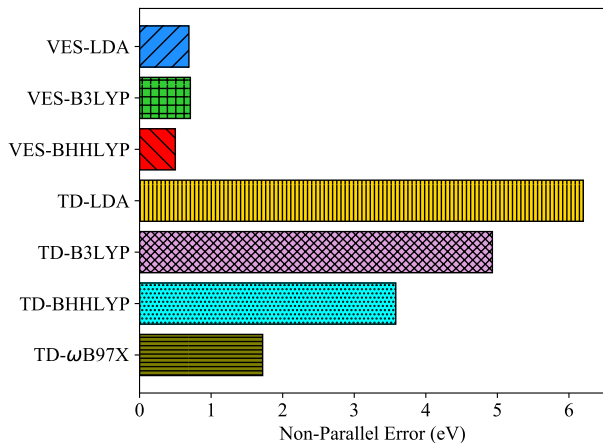


FIG. 9. Comparison of non-parallelity errors in the He $1s \rightarrow$ Be $2p$ CT excitation energy.

D. Rydberg Excitations

Unlike in CT excitations, it is not obvious that the ability of VES-DFT to address the EA/IP imbalance and orbital relaxations will be of great benefit in the context of Rydberg excitations. In these states, the challenge faced by TDDFT arises primarily from the failure of practical xc functionals to produce a potential that decays as $1/r$ at large distances, which is not the same as the failure of error cancellation that causes trouble in the CT case. However, work by Van Voorhis⁷⁴ has shown that although the ground state xc potential has little resemblance to the exact potential, the xc potential associated with an excited state density can behave much more sensibly at long distance. Thus, it is interesting to ask whether VES-DFT’s inherently excited state nature and its ability to relax the orbitals in an excited-state-specific manner may in practice lead to improvements for Rydberg states.

As an initial probe of this question, we have studied the $2s \rightarrow 3p$ excitation in the Ne atom. The excitation energy error v.s. EOM-CCSD is plotted in Figure 10. As expected, TDDFT drastically underestimates the excitation energy by as large as 8.21eV using LDA and 2.94eV using BHLYP. Notably, although our VES-DFT method is able to reduce the error of TDDFT by some amount, it is still very far from being quantitatively accurate. The most accurate functional in VES-DFT, the BHLYP functional, still underestimates the excitation energy by 2.74eV. Although there is no dipole change in this excitation, the charge deformation in Rydberg states is still large since the virtual orbitals are much more diffuse than and share little overlap with the occupied orbitals. Consequently, the averaged $\|\mathbf{X}\|$ is as large as 0.25, comparable to that of CT excitations. indicating that orbital relaxation is also important in Rydberg excitations.

As discussed in the previous subsection, the main source of error in VES-DFT is the self-interaction error with approximate xc functionals: The functional parametrized for the ground state is incapable of correcting the self-interaction er-

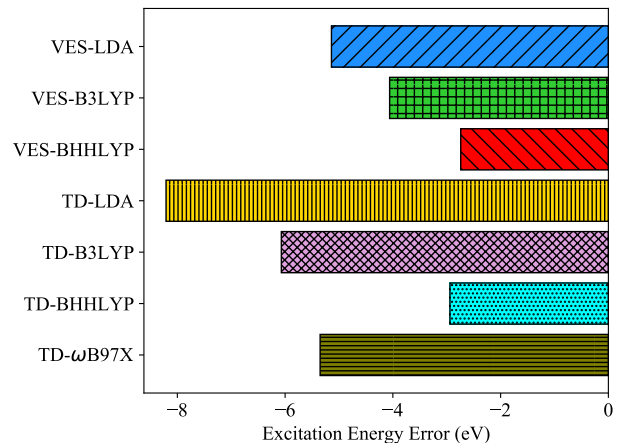


FIG. 10. Comparison of excitation energy error of the Ne $2s \rightarrow 3pz$ transition.

ror of the excited electron residing in virtual orbitals. This problem is not too concerning in valence excitations since the occupied and virtual orbitals have similar characters, and hence similar amount of self-interaction. Therefore thanks to error cancellation, balanced description between the ground and the excited states can still be achieved. However, in Rydberg states, the virtual orbitals are much more diffuse than the occupied orbitals. Consequently, the amount of SIEs left in $J[n]$ after adding the UEG exchange energy $E_x^{UEG}[n]$ to it, as in LDA, becomes clearly different in the occupied and virtual orbitals. This results in an unbalanced treatment between the ground and the excited state if one uses the same xc functionals for both states, leading to a large error in this Rydberg excitation energy. In future, testing asymptotically corrected functionals in VES-DFT would appear to be warranted.

V. CONCLUSIONS

We have presented an approach to excited states in DFT in which an approximated excited state variational principle is paired with a density functional energy expression. By adapting this expression for simple excited state wave function forms, this approach retains the Kohn-Sham advantage of evaluating the kinetic energy via a wave function that is qualitatively correct for the state in question. Indeed, in the same way that KS-DFT shows strong parallels to Hartree-Fock theory, VES-DFT is closely related to excited state mean field theory, which is a recently introduced approach to generalizing Hartree-Fock to excited states. Compared to TDDFT, whose reliance on linear response and the adiabatic approximation creates difficulties associated with orbital relaxations and the EA/IP imbalance, VES-DFT resolves both of these difficulties. In preliminary testing, this advantage results in dramatically improved energetics for charge transfer without a loss of accuracy in valence excitations, although Rydberg states remain a challenge in the theory’s current formulation.

Looking forward, there are many questions to answer if

VES-DFT is to become a modeling tool whose practical utility approaches current DFT methods. Somewhat unsurprisingly, given the open-shell nature of excited states, we find that functionals with higher-than-usual fractions of exact exchange are better at balancing self-interaction errors between the ground and excited state. This begs the question of whether the theory should even be defined as using the same functional for both states, and, if so, how to make a widely transferable choice for the exact exchange fraction. Of course, this is just one question in a much broader array of functional design issues, such as whether it would be advantageous to include range-separation or asymptotic corrections, which we have not yet explored. Functional design questions aside, there is also much work to do in improving the practical convergence properties of the optimization method. Although each step in the optimization has a cost that scales as a typical Fock build, the current approach often involves hundreds or even thousands of such steps, making its prefactor substantially higher than DIIS-accelerated implementations of ground state KS-DFT. As in excited state mean field theory, one wonders if there is an analogue of the self-consistent field optimization approach that would accelerate the optimization. Alternatively, a more careful examination of nonlinear optimization methods beyond the simple quasi-Newton approach used here may be fruitful. Given the exceptionally broad utility of current DFT methodology and the very promising early results showing how substantially VES-DFT can improve important excitation energies, we look forward to engaging with these questions in future.

ACKNOWLEDGMENTS

This work was supported by the National Science Foundation's CAREER program under Award Number 1848012. Calculations were performed using the Berkeley Research Computing Savio cluster.

- ¹R. G. Parr and W. Yang, *Density-functional theory of atoms and molecules* (Oxford University Press, New York, 1989).
- ²W. Kohn and L. J. Sham, "Self-consistent equations including exchange and correlation effects," *Phys. Rev.* **140**, A1133–A1138 (1965).
- ³E. Runge and E. K. U. Gross, "Density-functional theory for time-dependent systems," *Phys. Rev. Lett.* **52**, 997 (1984).
- ⁴M. Casida and M. Huix-Rotllant, "Progress in time-dependent density-functional theory," *Annu. Rev. Phys. Chem.* **63**, 287–323 (2012).
- ⁵C. A. Ullrich and Z.-h. Yang, "A brief compendium of time-dependent density-functional theory," *Braz. J. Phys.* **44**, 154–188 (2014).
- ⁶K. Burke, J. Werschnik, and E. K. U. Gross, "Time-dependent density functional theory: Past, present, and future," *J. Chem. Phys.* **123**, 062206 (2005).
- ⁷A. I. Krylov, "Equation-of-motion coupled-cluster methods for open-shell and electronically excited species: the Hitchhiker's guide to Fock space," *Annu. Rev. Phys. Chem.* **59**, 433–462 (2008).
- ⁸S. H. Vosko, L. Wilk, and M. Nusair, "Accurate spin-dependent electron liquid correlation energies for local spin density calculations: a critical analysis," *Can. J. Phys.* **58**, 1200–1211 (1980).
- ⁹Y. Zhao and D. G. Truhlar, "Applications and validations of the minnesota density functionals," *Chem. Phys. Lett.* **502**, 1–13 (2011).
- ¹⁰J.-D. Chai and M. Head-Gordon, "Systematic optimization of long-range corrected hybrid density functionals," *J. Chem. Phys.* **128**, 084106 (2008).
- ¹¹X. Zheng, T. Zhou, and W. Yang, "A nonempirical scaling correction

- approach for density functional methods involving substantial amount of hartree-fock exchange," *J. Chem. Phys.* **138**, 174105 (2013).
- ¹²Q. Zhao, E. I. Ioannidis, and H. J. Kulik, "Global and local curvature in density functional theory," *J. Chem. Phys.* **145**, 054109 (2016).
 - ¹³A. Bajaj, J. P. Janet, and H. J. Kulik, "Communication: Recovering the flat-plane condition in electronic structure theory at semi-local dft cost," *J. Chem. Phys.* **147**, 191101 (2017).
 - ¹⁴N. Mardirossian and M. Head-Gordon, "Thirty years of density functional theory in computational chemistry: an overview and extensive assessment of 200 density functionals," *Mol. Phys.* **115**, 2315–2372 (2017).
 - ¹⁵M. Petersilka, U. J. Grossmann, and E. K. U. Gross, "Excitation energies from time-dependent density-functional theory," *Phys. Rev. Lett.* **76**, 1212 (1995).
 - ¹⁶R. Bauernschmitt and R. Ahlrichs, "Treatment of electronic excitations within the adiabatic approximation of time dependent density functional theory," *Chem. Phys. Lett.* **256**, 454–464 (1996).
 - ¹⁷A. Dreuw, J. L. Weisman, and M. Head-Gordon, "Long-range charge-transfer excited states in time-dependent density functional theory require non-local exchange," *J. Chem. Phys.* **119**, 2943–2946 (2003).
 - ¹⁸H. Nitta and I. Kawata, "A close inspection of the charge-transfer excitation by tddft with various functionals: An application of orbital- and density-based analyses," *Chem. Phys.* **405**, 93–99 (2012).
 - ¹⁹J. J. Eriksen, S. P. Sauer, K. V. Mikkelsen, O. Christiansen, H. J. A. Jensen, and J. Kongsted, "Failures of tddft in describing the lowest intramolecular charge-transfer excitation in para-nitroaniline," *Mol. Phys.* **111**, 1235–1248 (2013).
 - ²⁰Y. Yang, H. Van Aggelen, and W. Yang, "Double, Rydberg and charge transfer excitations from pairing matrix fluctuation and particle-particle random phase approximation," *J. Chem. Phys.* **139** (2013), 10.1063/1.4834875.
 - ²¹M. E. Casida and D. R. Salahub, "Asymptotic correction approach to improving approximate exchange-correlation potentials: Time-dependent density-functional theory calculations of molecular excitation spectra," *J. Chem. Phys.* **113**, 8918–8935 (2000).
 - ²²R. Van Meer, O. V. Gritsenko, and E. J. Baerends, "Physical meaning of virtual kohn-sham orbitals and orbital energies: An ideal basis for the description of molecular excitations," *J. Chem. Theory Comput.* **10**, 4432–4441 (2014).
 - ²³A. Dreuw and M. Head-gordon, "Single-Reference ab Initio Methods for the Calculation of Excited States of Large Molecules," *Sciences-New York*, 4009–4037 (2005).
 - ²⁴P. Elliott, S. Goldson, C. Canahui, and N. T. Maitra, "Perspectives on double-excitations in tddft," *Chem. Phys.* **391**, 110 – 119 (2011).
 - ²⁵O. Gritsenko and E. J. Baerends, "Asymptotic correction of the exchange-correlation kernel of time-dependent density functional theory for long-range charge-transfer excitations," *J. Chem. Phys.* **121**, 655–660 (2004).
 - ²⁶J. D. Chai and M. Head-Gordon, "Long-range corrected hybrid density functionals with damped atom-atom dispersion corrections," *Phys. Chem. Chem. Phys.* **10**, 6615–6620 (2008).
 - ²⁷J. D. Chai and M. Head-Gordon, "Systematic optimization of long-range corrected hybrid density functionals," *J. Chem. Phys.* **128**, 0–15 (2008).
 - ²⁸N. Mardirossian and M. Head-Gordon, "ωB97X-V: A 10-parameter, range-separated hybrid, generalized gradient approximation density functional with nonlocal correlation, designed by a survival-of-the-fittest strategy," *Phys. Chem. Chem. Phys.* **16**, 9904–9924 (2014).
 - ²⁹N. Mardirossian and M. Head-Gordon, "ω B97M-V: A combinatorially optimized, range-separated hybrid, meta-GGA density functional with VV10 nonlocal correlation," *J. Chem. Phys.* **144** (2016), 10.1063/1.4952647.
 - ³⁰R. Peverati and D. G. Truhlar, "Improving the accuracy of hybrid meta-gga density functionals by range separation," *J. Phys. Chem. Lett.* **2**, 2810–2817 (2011).
 - ³¹Y.-S. Lin, C.-W. Tsai, G.-D. Li, and J.-D. Chai, "Long-range corrected hybrid meta-generalized-gradient approximations with dispersion corrections," *J. Chem. Phys.* **136**, 154109 (2012).
 - ³²T. Stein, L. Kronik, and R. Baer, "Prediction of charge-transfer excitations in coumarin-based dyes using a range-separated functional tuned from first principles," *J. Chem. Phys.* **131**, 244119 (2009).
 - ³³L. Kronik, T. Stein, S. Refaely-Abramson, and R. Baer, "Excitation gaps of finite-sized systems from optimally tuned range-separated hybrid functionals," *J. Chem. Theory Comput.* **8**, 1515–1531 (2012).

- ³⁴N. T. Maitra, F. Zhang, R. J. Cave, and K. Burke, "Double excitations within time-dependent density functional theory linear response," *J. Chem. Phys.* **120**, 5923 (2004).
- ³⁵N. T. Maitra, "Perspective: Fundamental aspects of time-dependent density functional theory," *J. Chem. Phys.* **144**, 220901 (2016).
- ³⁶Y. C. Park, M. Krykunov, and T. Ziegler, "On the relation between adiabatic time dependent density functional theory (TDDFT) and the Δ SCF-DFT method. introducing a numerically stable Δ SCF-DFT scheme for local functionals based on constricted variational DFT," *Mol. Phys.* **113**, 1636–1647 (2015).
- ³⁷T. Ziegler, M. Seth, M. Krykunov, J. Autschbach, and F. Wang, "On the relation between time-dependent and variational density functional theory approaches for the determination of excitation energies and transition moments," *J. Chem. Phys.* **130**, 154102 (2009).
- ³⁸T. Ziegler, M. Seth, M. Krykunov, and J. Autschbach, "A revised electronic hessian for approximate time-dependent density functional theory," *J. Chem. Phys.* **129**, 184114 (2008).
- ³⁹L. Zhao and E. Neuscamman, "An Efficient Variational Principle for the Direct Optimization of Excited States," *J. Chem. Theory Comput.* **12**, 3436–3440 (2016), arXiv:1508.06683.
- ⁴⁰H.-Z. Ye, M. Welborn, N. D. Ricke, and T. Van Voorhis, " σ -scf: A direct energy-targeting method to mean-field excited states," *J. Chem. Phys.* **147**, 214104 (2017).
- ⁴¹J. A. Shea and E. Neuscamman, "Communication: A mean field platform for excited state quantum chemistry," *J. Chem. Phys.* **149** (2018).
- ⁴²M. Abadi, A. Agarwal, P. Barham, E. Brevdo, Z. Chen, C. Citro, G. S. Corrado, A. Davis, J. Dean, M. Devin, S. Ghemawat, I. Goodfellow, A. Harp, G. Irving, M. Isard, Y. Jia, R. Jozefowicz, L. Kaiser, M. Kudlur, J. Levenberg, D. Mané, R. Monga, S. Moore, D. Murray, C. Olah, M. Schuster, J. Shlens, B. Steiner, I. Sutskever, K. Talwar, P. Tucker, V. Vanhoucke, V. Vasudevan, F. Viégas, O. Vinyals, P. Warden, M. Wattenberg, M. Wicke, Y. Yu, and X. Zheng, "TensorFlow: Large-scale machine learning on heterogeneous systems," (2015), software available from tensorflow.org.
- ⁴³J. Nocedal, "Updating quasi-newton matrices with limited storage," *Math. Comp.* **35**, 773 – 782 (1980).
- ⁴⁴S. Hirata, M. Head-Gordon, and R. J. Bartlett, "Configuration interaction singles, time-dependent Hartree-Fock, and time-dependent density functional theory for the electronic excited states of extended systems," *J. Chem. Phys.* **111**, 10774–10786 (1999).
- ⁴⁵C. Lee, W. Yang, and R. G. Parr, "Development of the Colle-Salvetti correlation-energy formula into a functional of the electron density," *Phys. Rev. B* **162**, 165–169 (1988).
- ⁴⁶A. D. Becke, "Density-functional exchange-energy approximation with correct asymptotic behavior," *Phys. Rev. A* **38**, 3098 (1988).
- ⁴⁷A. D. Becke, "A new inhomogeneity parameter in density-functional theory," *J. Chem. Phys.* **109**, 2092–2098 (1998).
- ⁴⁸A. D. Becke, "Density-functional thermochemistry. III. The role of exact exchange," *J. Chem. Phys.* **98**, 5648–5652 (1993).
- ⁴⁹J. Gräfenstein and D. Cremer, "The combination of density functional theory with multi-configuration methods - CAS-DFT," *Chem. Phys. Lett.* **316**, 569–577 (2000).
- ⁵⁰C. M. Marian, A. Heil, and M. Kleinschmidt, "The DFT/MRCI method," *Wiley Interdiscip. Rev. Comput. Mol. Sci.* **9**, e1394 (2019).
- ⁵¹G. L. Manni, R. K. Carlson, S. Luo, D. Ma, J. Olsen, D. G. Truhlar, and L. Gagliardi, "Multiconfiguration pair-density functional theory," *J. Chem. Theory Comput.* **10**, 3669–3680 (2014).
- ⁵²R. K. Carlson, D. G. Truhlar, and L. Gagliardi, "Multiconfiguration pair-density functional theory: A fully translated gradient approximation and its performance for transition metal dimers and the spectroscopy of $Re_2Cl_8^{-2}$," *J. Chem. Theory Comput.* **11**, 4077–4085 (2015).
- ⁵³P. Sharma, V. Bernales, S. Knecht, D. Truhlar, and L. Gagliardi, "Density matrix renormalization group pair-density functional theory (DMRG-PDFT): singlet-triplet gaps in polyacenes and polyacetylenes," *Chem. Sci.* **10**, 1716 (2019).
- ⁵⁴V. N. Staroverov and E. R. Davidson, "Charge densities for singlet and triplet electron pairs," *Int J. Quantum Chem.* **77**, 651–660 (1999).
- ⁵⁵T. Ziegler, A. Rauk, and E. J. Baerends, *Theor. Chim. Acta* **43**, 261 (1977).
- ⁵⁶A. T. B. Gilbert, N. A. Besley, and P. M. W. Gill, "Self-Consistent Field Calculations of Excited States Using the Maximum Overlap Method," *J. Phys. Chem. A* **112(50)**, 13164–13171 (2008).
- ⁵⁷N. A. Besley, A. T. B. Gilbert, and P. M. W. Gill, *J. Chem. Phys.* **130**, 124308 (2009).
- ⁵⁸T. Kowalczyk, T. Tsuchimochi, P. T. Chen, L. Top, and T. Van Voorhis, "Excitation energies and Stokes shifts from a restricted open-shell Kohn-Sham approach," *J. Chem. Phys.* **138** (2013).
- ⁵⁹D. Hait, T. Zhu, D. P. McMahon, and T. Van Voorhis, "Prediction of excited-state energies and singlet-triplet gaps of charge-transfer states using a restricted open-shell Kohn-Sham approach," *J. Chem. Theory Comput.* **12**, 3353–3359 (2016).
- ⁶⁰B. Kaduk, T. Kowalczyk, and T. V. Voorhis, "Constrained density functional theory," *Chem. Rev.* **112**, 321–370 (2012).
- ⁶¹Q. Wu and T. V. Voorhis, "Constrained density functional theory and its application in long-range electron transfer," *J. Chem. Theory Comput.* **2**, 765–774 (2006).
- ⁶²Q. Wu and T. V. Voorhis, "Extracting electron transfer coupling elements from constrained density functional theory," *J. Chem. Phys.* **125**, 164105 (2006).
- ⁶³Q. Wu and T. V. Voorhis, "Direct calculation of electron transfer parameters through constrained density functional theory," *J. Phys. Chem. A* **110**, 9212–9218 (2006).
- ⁶⁴B. Kaduk and T. V. Voorhis, "Communication: Conical intersections using constrained density functional theory–configuration interaction," *J. Chem. Phys.* **133**, 061102 (2010).
- ⁶⁵Q. Sun, T. C. Berkelbach, N. S. Blunt, G. H. Booth, S. Guo, Z. Li, J. Liu, J. D. McClain, E. R. Sayfutyarova, S. Sharma, S. Wouters, and G. K. L. Chan, "PySCF: the Python-based simulations of chemistry framework," *Wiley Interdiscip. Rev. Comput. Mol. Sci.* **8** (2018).
- ⁶⁶V. I. Lebedev and D. N. Laikov, "A quadrature formula for the sphere of the 131st algebraic order of accuracy," *Dokl. Math.* **59**, 477–481 (1999).
- ⁶⁷Y. Shao, Z. Gan, E. Epifanovsky, A. T. Gilbert, M. Wormit, J. Kussmann, A. W. Lange, A. Behn, J. Deng, X. Feng, D. Ghosh, M. Goldey, P. R. Horn, L. D. Jacobson, I. Kaliman, R. Z. Khaliullin, T. Kuś, A. Landau, J. Liu, E. I. Proynov, Y. M. Rhee, R. M. Richard, M. A. Rohrdanz, R. P. Steele, E. J. Sundstrom, H. L. W. III, P. M. Zimmerman, D. Zuev, B. Albrecht, E. Alguire, B. Austin, G. J. O. Beran, Y. A. Bernard, E. Berquist, K. Brandhorst, K. B. Bravaya, S. T. Brown, D. Casanova, C.-M. Chang, Y. Chen, S. H. Chien, K. D. Closser, D. L. Crittenden, M. Diedenhofen, R. A. D. Jr., H. Do, A. D. Dutoi, R. G. Edgar, S. Fatehi, L. Fusti-Molnar, A. Ghysels, A. Golubeva-Zadorozhnaya, J. Gomes, M. W. Hanson-Heine, P. H. Harbach, A. W. Hauser, E. G. Hohenstein, Z. C. Holden, T.-C. Jagau, H. Ji, B. Kaduk, K. Khistyayev, J. Kim, J. Kim, R. A. King, P. Klunzinger, D. Kosenkov, T. Kowalczyk, C. M. Krauter, K. U. Lao, A. D. Laurent, K. V. Lawler, S. V. Levchenko, C. Y. Lin, F. Liu, E. Livshits, R. C. Lochan, A. Luenser, P. Manohar, S. F. Manzer, S.-P. Mao, N. Mardirossian, A. V. Marenich, S. A. Maurer, N. J. Mayhall, E. Neuscamman, C. M. Oana, R. Olivares-Amaya, D. P. O'Neill, J. A. Parkhill, T. M. Perrine, R. Peverati, A. Prociuk, D. R. Rehn, E. Rosta, N. J. Russ, S. M. Sharada, S. Sharma, D. W. Small, A. Sodt, T. Stein, D. Stück, Y.-C. Su, A. J. Thom, T. Tsuchimochi, V. Vanovschi, L. Vogt, O. Vydrov, T. Wang, M. A. Watson, J. Wenzel, A. White, C. F. Williams, J. Yang, S. Yeganeh, S. R. Yost, Z.-Q. You, I. Y. Zhang, X. Zhang, Y. Zhao, B. R. Brooks, G. K. Chan, D. M. Chipman, C. J. Cramer, W. A. G. III, M. S. Gordon, W. J. Hehre, A. Klamt, H. F. S. III, M. W. Schmidt, C. D. Sherrill, D. G. Truhlar, A. Warshel, X. Xu, A. Aspuru-Guzik, R. Baer, A. T. Bell, N. A. Besley, J.-D. Chai, A. Dreuw, B. D. Dunietz, T. R. Furlani, S. R. Gwaltney, C.-P. Hsu, Y. Jung, J. Kong, D. S. Lambrecht, W. Liang, C. Ochsenfeld, V. A. Rassolov, L. V. Slipchenko, J. E. Subotnik, T. V. Voorhis, J. M. Herbert, A. I. Krylov, P. M. Gill, and M. Head-Gordon, "Advances in molecular quantum chemistry contained in the q-chem 4 program package," *Mol. Phys.* **113**, 184–215 (2015).
- ⁶⁸P. J. Knowles, F. R. Manby, H.-J. Werner, G. Knizia, and M. Schütz, "Molpro: a general-purpose quantum chemistry program package," *Wiley Interdiscip. Rev. Comput. Mol. Sci.* **2**, 242–253 (2011).
- ⁶⁹T. H. Dunning, "Gaussian basis sets for use in correlated molecular calculations. I. the atoms boron through neon and hydrogen," *J. Chem. Phys.* **90**, 1007 (1988).
- ⁷⁰R. A. Kendall, T. H. Dunning, and R. J. Harrison, "Electron affinities of the first-row atoms revisited. Systematic basis sets and wave functions," *J. Chem. Phys.* **96**, 6796 (1992).
- ⁷¹W. J. Hehre, R. Ditchfield, and J. A. Pople, "Self-consistent molecular

- orbital methods. XII. further extensions of Gaussian-type basis sets for use in molecular orbital studies of organic molecules," *J. Chem. Phys.* **56**, 2257 (1972).
- ⁷²Y. Zhao and D. G. Truhlar, "Density functional for spectroscopy: No long-range self-interaction error, good performance for Rydberg and charge-transfer states, and better performance on average than B3LYP for ground states," *J. Phys. Chem. A* **110**, 13126–13130 (2006).
- ⁷³E. J. Baerends, O. V. Gritsenko, and R. van Meer, "The Kohn-Sham gap, the fundamental gap and the optical gap: the physical meaning of occupied and virtual Kohn-Sham orbital energies," *Phys. Chem. Chem. Phys.* **15**, 16408 (2013).
- ⁷⁴C.-L. Cheng, Q. Wu, and T. V. Voorhis, "Rydberg energies using excited state density functional theory," *J. Chem. Phys.* **129**, 124112 (2008).